CHAPTER V
EFFECT OF TRANSITION METALS ON THE ELECTRICAL CONDUCTIVITY RESPONSE OF DPPV/ZEOLITE Y COMPOSITES TOWARDS KETONE VAPORS

5.1 Abstract

Doped poly(p-phenylene vinylene) (DPPV) was mixed with modified zeolite Y to improve the selective and sensitive response of zeolite Y toward three different ketone vapors (acetone, MEK, and MIBK) known as the toxic components. Zeolite Y (Si/Al=5.1 and Na^{+}) or NaY was ion exchanged with transition cations: Cu^{2+}; Ni^{2+}; and Fe^{2+} at 80% cation exchanged to prepare 80CuNaY, 80NiNaY, and 80FeNaY. In this work, the effects of transition cations, ketone vapor types, and ketone vapor concentration were systematically investigated. The highest electrical conductivity response and sensitivity toward acetone vapor at the vapor concentration of 30000 ppm was obtained with 80CuNaY, whereas 80FeNaY showed the lowest values due to the electrostatic interaction between the zeolite framework and the cation. DPPV was mixed with 80CuNaY and exposed to the three ketone vapors. The electrical conductivity response and sensitivity of the composites towards acetone exhibited the highest values whereas with MIBK they showed the lowest value. After mixing 80CuNaY with dPPV, the minimum vapor concentration towards acetone vapor decreased from 9 ppm to 5 ppm. The response of the composite was irreversible as evidenced by FTIR and AFM techniques.

Keywords: Conducting Materials, Ketones, Sensors and Zeolites

5.2 Introduction

Air pollution results mainly from the usage of petroleum and petrochemical products. The concerned processes generate toxic gases and chemical vapors. Therefore, the development of toxic gas and vapor detection materials is always needed which possess high response, good selectivity, fast recovery, and low cost.

Many types of material have been explored and used as gas sensors: conducting polymers (Heeger *et al.*, 1998; Benvenho *et al.*, 2008; Yung *et al.*, 2008; Pirsa *et al.*, 2012); porous materials (Vijaya *et al.*, 2008; Varsani *et al.*, 2011; Satsuma *et al.*, 2012; Urbiztondo *et al.*, 2012); and metal oxides (Tang *et al.*, 2008; Ayad *et al.*, 2009; Chang *et al.*, 2011; Gao *et al.*, 2011; Hung *et al.*, 2011).

Zeolite is one of the porous materials which are widely used as sensor materials such as faujasite (zeolite X and zeolite Y), ZSM-5, and mordenite due to its adsorption and separation properties. The structure of zeolite is the framework of hydrated aluminosilicates consisting of group I and II elements. The zeolite framework contains channels and interconnected voids which are occupied by water and cations. Zeolites are known to provide high chemical stability, high porosity, high surface area, high selectivity, and adsorption properties. Nevertheless, zeolites still possess low electrical conductivity values. The processes for improving the electrical conductivity of a zeolite are through adjusting the Si/Al ratio of zeolite, the ion exchange process, and blending with conductive polymers (Auerbach *et al.*, 2003; Vijaya *et al.*, 2008; Satsuma *et al.*, 2012; Urbiztondo *et al.*, 2012; Varsani *et al.*, 2011). The ion exchanged processes with alkaline, alkaline earth, and transition metals are expected to change the response and selectivity properties of zeolites. The ion exchange process combined with blending a conductive polymer into the zeolite matrix have been shown to effectively improve the electrical conductivity of the zeolite for detecting toxic gases and chemical vapors (Auerbach *et al.*, 2003; Ruangchuay *et al.*, 2004; Li *et al.*, 2006; Yang *et al.*, 2007; Wannatong *et al.*, 2008; Vijaya *et al.*, 2008; Thongchai *et al.*, 2009; Arvand *et al.*, 2011; Varsani *et al.*, 2011; Chanthaanont *et al.*, 2012; Ji *et al.*, 2012; Li *et al.*, 2012; Satsuma *et al.*, 2012; Urbiztondo *et al.*, 2012).

Conductive polymers (CPs) are the other type of materials which can be used as gas sensing materials as they show the high electrical conductivity, magnetic, and optical properties. One of the conductive polymers which has been widely used in the gas sensing application is Poly(p-phenlene vinylene) or PPV because it has a high electrical conductivity, good mechanical properties, good chemical stability, and ease in synthesizing (Wessling *et al.*, 1968; Ahlskog *et al.*, 1997; Kamonsawas *et al.*, 2010). A positive or negative response of doped PPV or dPPV depends on the

electrophilic or nucleophilic nature of the gases or chemical vapors. Although dPPV exhibits a high electrical conductivity value, its selectivity and adsorption properties are still poor towards a particular chemical vapor. Previous work has combined the best characteristics of zeolites and the high electrical properties of the conductive polymers to improve the selective, adsorptive, and electronic properties toward gases and vapors (Kamonsawas *et al.*, 2010; Chanthaanont *et al.*, 2012).

In this work, zeolite Y was ion exchanged process with the transition cations (Cu^{2+}, Ni^{2+}, and Fe^{2+}) to improve the electrical conductivity response of zeolite Y (Si/Al=5.1) towards acetone vapor under the effects of transition metal and vapor concentration. The electrical conductivity responses of the composites between zeolite Y and dPPV towards three different types of ketone vapors (acetone, MEK, and MIBK) were also investigated. The interaction between the active site of the sensing materials and the chemical vapors were investigated by FTIR and AFM techniques and shall be reported here.

5.3 Experimental

5.3.1 Materials Preparation

5.3.1.1 Synthesis of Poly(p-Phenylene Vinylene) or PPV and Doping Process

Synthesis of PPV was prepared via the Wessling route (Wessling *et al.*, 19680). The α, α'-dichloro-p-xylene (Aldrich) and tetrahydrothio phene (Aldrich) were raw materials to synthesize the p-xylene-bis (tetrahydro thio-phenium chloride) monomer. The polymerization step was induced by the sodium hydroxide to form a precursor polymer. PPV was obtained by heating the precursor polymer in the vacuum oven at 180 °C for 6 h (Wessling *et al.*, 19680). Adding the solution of 18 M sulfuric acid at the mole ratio of 1:100 (PPV repeating units and sulfuric acid to the polymer powder and the change of the polymer color from bright yellow to black brown was observed which indicated the complete doping process (Ahlskog *et al.*, 1997).

5.3.1.2 The Cation Exchange Process

The ion exchanged process was carried out by using the zeolite Y (Si/Al=5.1 and Na^+) or NaY purchased from Zeolyst. The preparations of the zeolite Y (Si/Al=5.1, 20% mole of Na^+, and 80% mole of Cu^{2+}) or 80CuNaY, the zeolite Y (Si/Al=5.1, 20% mole of Na^+, and 80% mole of Ni^{2+}) or 80NiNaY, and the zeolite Y (Si/Al=5.1, 20% mole of Na^+ and 80% mole of Fe^{2+}) or 80FeNaY were by adding the 0.1 M solution of $CuCl_2$, $NiCl_2$, and $FeSO_4$ into 5 grams of NaY and stirred at 25 °C for 24 h. Then, the zeolite samples were filtered and washed with DI-water for 5 times (Li *et al.*, 2012; Thuwachaosuan *et al.*, 2007).

5.3.1.3 Preparation of dPPV_Zeolilte Y Pellet

DPPV was mixed into the zeolite Y matrix (80CuNaY, 80NiNaY, 80FeNaY, and NaY). The composites between zeolite Y and dPPV were prepared by physical blending at the percentage volume of dPPV of 10% v/v. The hydraulic press was used to form composite pellets at the pressure of 6 kN.

5.3.2 Characterization of PPV, dPPV and Composite

The surface area analysis (Sorptomatic-1990) was used to determine the median pore sizes and the surface areas of the zeolite Y. The percentage of ion exchanged was measured by an atomic adsorption spectrophotometer (Spectra A300, Varian). A FT-IR spectrometer (Inclolet, model FRA 106/S) was used to characterize functional groups of PPV, dPPV and the interaction between the chemical vapors and the active site of gas sensing materials. The morphology of PPV, dPPV, zeolite Y, and the 10% v/v of dPPV on the composites or dPPV_[90]80CuNaY, and the dispersion of the conductive polymer particles in the zeolite Y, were investigated a scanning electron microscope or SEM (Hitachi, SU1510) at the magnifications of 1000x and 5000x and at 10 kV. The specific electrical conductivity was measured by a custom man made two-point probe with a linear geometric array connected to a voltage supplier (Keithley, 6517A). Atomic force microscope or AFM (Park systems, XE-100) was used to characterize the phase changes during the acetone exposure.

5.3.3 Electrical Conductivity and Chemical Vapor Detection

A voltage supplier (Keithley, 6517A) was connected to a custom made 2-point probe to measure the electrical conductivity of the gas sensing materials under the condition of air, N_2, and chemical vapors where the voltage was varied and the current was measured. The electrical conductivity was calculated by equation 5.1.

$$\sigma = (I/KVt) \qquad 5.1$$

where I is the measured current (A), V is the applied voltage (V), t is the thickness, and K is the geometric correction factor of the two-point probe which determined by calibrating the probe with a silicon wafer possessing a known resistivity value.

The flow system of gas detection unit was connected to the custom made 2-point probe and the voltage supplier (Keithley, 6517A) was used to monitor the change in the electrical conductivity during the chemical vapor exposure. The chemical vapors in this work were acetone, MEK, and MIBK. All of chemicals were purchased from Labscan (AR grade). The chemical vapors were generated by the flow system at the vapor concentrations of 30000 ppm (3% v/v), 3000 ppm (0.3% v/v), 300 ppm (0.03% v/v), 30 ppm (0.003% v/v), and 10 ppm (0.001% v/v) in N_2 gas. The surface cleaning gas which vaporized the chemical solvents was nitrogen (N_2, TIG). All chemicals were used without further purifications. Air and moisture were evacuated from the chemical chamber until the steady state was obtained and nitrogen was injected as into the chemical camber. When the electrical conductivity in N_2 gas reached the steady state, the electrical conductivity was recorded as $\sigma_{N2,\ \text{before exposure}}$. Before injecting the chemical vapor into the chemical chamber, nitrogen gas was evacuated first and chemical vapor was later injected into the chamber. At the steady state, the electrical conductivity was recorded as $\sigma_{\text{chemical vapor}}$. The chemical vapor was removed by the vacuum pump and then N_2 was injected into the chamber, and the electrical conductivity was measured as $\sigma_{N2,\ \text{after exposure}}$. The electrical conductivity response and sensitivity of the composites were calculated by following the equations 5.2 and 5.3.

$$\Delta\sigma = \sigma_{\text{chemical vapor}} - \sigma_{N2,\ \text{before exposure}} \qquad 5.2$$

$$\text{Sensitivity} = \Delta\sigma / \sigma_{N_2\ \textit{before exposure}} \qquad 5.3$$

where $\Delta\sigma$ is the difference in the specific electrical conductivity (S/cm), $\sigma_{N2,\ before\ exposure}$ is the specific electrical conductivity in N_2 before exposure (S/cm), and $\sigma_{chemical\ vapor}$ is the specific electrical conductivity under chemical vapor exposure (S/cm) (Wannatong *et al.*, 2008; Kamonsawas *et al.*, 2010).

5.4 Results and Discussion

5.4.1 Characterization of dPPV, Modified Zeolite Y and Its Composite

Table 5.1 shows the analytical data and the electrical conductivity values of the modified zeolite Y which was ion exchanged with three different transition cations.

Zeolite Y (Si/Al=5.1 and Na^+) or NaY was ion exchanged with Cu^{2+}, Ni^{2+}, and Fe^{2+}. The amount of cation exchange was determined by the atomic adsorption spectrophotometer (AAS) in terms of cation mole percentage. From the previous work (Soontornworajit *et al.*, 2007; Thuwachaosuan *et al.*, 2007; Kamonsawas *et al.*, 2010), the % mole cation is defined as the ratio of Cu^{2+}, Ni^{2+}, and Fe^{2+} divided by the sums of moles of individual cations and multiplied by 100. The cation mole percentages of Cu^{2+}, Ni^{2+}, and Fe^{2+} are 79%, 84%, and 90%, respectively for the exchanged time of 24 h as tabulated in Table 5.1 (Auerbach *et al.*, 2003; Soontornworajit *et al.*, 2007; Thuwachaosuan *et al.*, 2007).

Figure 5.1 shows the morphology of dPPV, 80CuNaY, and the composites. The morphology of dPPV and 80CuNaY are shown in Figures 5.1a and 5.1b at the magnification of 5000x and 10kV. Figure 5.1c shows the morphology of the composites between 10% v/v of dPPV and 80CuNaY or dPPV_[90]80CuNaY at magnification of 5000x. After mixing 10% v/v of dPPV into the 80CuNaY matrix, the morphology of the composite appears as a nearly homogenous mixture.

The electrical conductivity values of 80CuNaY, 80NiNaY, NaY, and 80FeNaY under ambient condition are $5.67 \times 10^{-3} \pm 7.08 \times 10^{-5}$ S.cm^{-1}, $3.51 \times 10^{-3} \pm 1.15 \times 10^{-6}$ S.cm^{-1}, $2.50 \times 10^{-3} \pm 2.51 \times 10^{-5}$ S.cm^{-1}, and $2.44 \times 10^{-3} \pm 1.66 \times 10^{-5}$ S.cm^{-1}, respectively as tabulated in Table 5.1. The electrical conductivity of the zeolite depends on the cationic radii. 80CuNaY shows a higher value of the electrical conductivity than 80NiNaY and 80FeNaY, respectively because of the charge

balanced ion size. The size of Cu^{2-} (0.87 Å) are larger than those Ni^{2+} (0.83 Å) and Fe^{2+} (0.75 Å), respectively. The large cation size leads to a reduction in the electrostatic force of the zeolite framework and the increase in the proton mobility along the zeolite structure (McKeen *et al.*, 2009; Yimlamai *et al.*, 2011; Kamonsawas *et al.*, 2012). In addition, the electron orbitals of the cation in the zeolite framework are other factors affecting the electrical conductivity values. Figure 2 shows the electron orbitals of Cu^{2+}, Ni^{2+}, and Fe^{2+}. The electron orbital of Cu^{2+}, Ni^{2+}, and Fe^{2+} are in the unfilled state in the 3d orbitals and the unfilled electron state of Cu^{2+}, Ni^{2+}, and Fe^{2+} are 1, 2, and 4 respectively as shown in Figure 5.2. Therefore, Cu^{2+} is capable of rapidly accepting electrons and induces the highest electrical conductivity value. In the case of Na^{+} which is an alkaline cation, the electrical conductivity of NaY is lower than those 80CuNaY and 80 NiNaY due to the void size within the zeolite. Typically, two Na^{+} are replaced with one Cu^{2+} where the ionic radii of Na^{+} and Cu^{2+} are 1.16 Å and 0.87 Å, respectively. After replacing Na^{+} with Cu^{2+}, this results in increasing the void within the zeolite framework and leads to the increase in the proton mobility along the zeolite framework (Thongchai *et al.*, 2009; Ji *et al.*, 2012). The electrical conductivity sensitivity values of dPPV, zeolite Y and composites towards three different ketone vapors are shown and discussed next.

5.4.2 The Temporal Response of Zeolite Y and Composites

Table 5.2 lists the inductions time (Ti) and recovery time (Tr) of zeolite Y and the composites. The induction time of 80CuNaY, 80NiNaY, NaY, and 80FeNaY when exposed to acetone vapor at the vapor concentration of 30000 ppm, 25 °C and 1 atm are 38 ± 1, 40 ± 1, 42 ± 2, and 45 ± 1 min, respectively. The recovery times are 31 ± 2, 32 ± 1, 27 ± 2, and 38 ± 1 min, respectively. Generally, the induction time is dependent on the cation type which possesses different EN values, cationic radii, and electron configuration properties (Shannon *et al.*, 1976; Li *et al.*, 2006; Ji *et al.*, 2012). Cu^{2+} in the zeolite framework has the electron configuration which remains one electron unfilled state in 3d orbital, resulting in an increase in the adsorption property, as shown in Figure 5.2 (Shannon *et al.*, 1976; Li *et al.*, 2006; Ji *et al.*, 2012). Therefore, 80CuNaY shows the shortest induction time.

In the case of Na^+, it is an alkaline cation which has a lower EN value (0.93) than Cu^{2+} (1.372) and Ni^{2+} (1.367). Therefore, Na^+ also shows the longer induction time than Cu^{2+} and Ni^{2+}. For the recovery time, NaY takes the shortest time due to its EN value. The En value of Na^+ (0.93) is considerably lower than Cu^{2+} (1.372), Ni^{2+} (1.367), and Fe^{2+} (1.292), respectively. The low EN value suggests a weaker interaction between the active site and the chemical vapor. Therefore, 80CuNaY is chosen for the further study under the effects of ketone type and dPPV. The induction and recovery times of 80CuNaY are investigated under the effect of ketone type. The induction times of 80CuNaY are 38 ± 1, 35 ± 2, and 18 ± 2 min, respectively and the recovery times of this sample are 31 ± 2, 13 ± 1, and 12 ± 2 min, respectively under the exposure of acetone, MEK, and MIBK at the vapor concentration of 30,000 ppm The induction and recovery times depend on the ketone molecular size. A solvent molecule with a smaller size can easily penetrate into the zeolite framework and takes a longer time. The size of acetone is smaller than those of MEK and MIBK molecules. Hence, 80CuNaY sample when exposed to acetone vapor takes the longer time to reach a steady state than MEK (Ji *et al.*, 2012; Kamonsawas *et al.*, 2012).

dPPV is mixed with 80CuNaY at the ratio of 10% PPV and exposed to acetone vapor at the vapor concentration of 30000 ppm, 25 °C and 1 atm. The induction time of dPPV_[90]80CuNaY is 36 ± 1 and the recovery time is 26 ± 1. After mixing dPPV into the 80CuNaY matrix, the induction and the recovery time decrease due to the available active site property change in the composite system. Other ketone types show similar results (Soontornworajit *et al.*, 2007; Thuwachaosuan *et al.*, 2007; Thongchai *et al.*, 2010; Chanthaanont *et al.*, 2012; Kamonsawas *et al.*, 2012).

5.4.3 The Response of Zeolite Y, dPPV and Composites

5.4.3.1 Effect of Transition Cations

The electrical conductivity response and the sensitivity values of 80CuNaY, 80NiNaY, NaY, and 80FeNaY are shown in Figure 5.3 and tabulated in Table 5.3. Zeolite Y (Si/Al=5.1 and Na^+) or NaY was ion exchanged with Cu^{2+},

Ni^{2+}, and Fe^{2+} at 80% mole to investigate the effect of transition metals toward acetone vapor at the vapor concentrations of 30000, 3000, 300, 30, and 10 ppm.

The electrical conductivity response of 80FeNaY, NaY, 80NiNaY, and 80CuNaY in acetone exposure at the vapor concentration of 30000 ppm are $1.49 \times 10^{-04} \pm 2.16 \times 10^{-06}$, $3.23 \times 10^{-04} \pm 9.95 \times 10^{-05}$, $4.62 \times 10^{-04} \pm 8.06 \times 10^{-06}$, and $6.74 \times 10^{-04} \pm 2.04 \times 10^{-05}$ $S.cm^{-1}$, respectively. The electrical conductivity sensitivities are $2.38 \times 10^{-01} \pm 1.66 \times 10^{-02}$, $2.64 \times 10^{-01} \pm 2.05 \times 10^{-02}$, $3.53 \times 10^{-01} \pm 1.93 \times 10^{-02}$, and $5.00 \times 10^{-01} \pm 2.20 \times 10^{-02}$, respectively. The electrical conductivity response increases with increasing cationic radii. The large cation size decreases the electrostatic interaction between the cation and the zeolite framework and thus increases the proton mobility along the zeolite structure (McKeen *et al.*, 2009; Yimlamai *et al.*, 2011; Kamonsawas *et al.*, 2012). The cation radii of Fe^{2+}, Ni^{2+}, and Cu^{2+} are 0.75 Å, 0.83 Å, and 0.87 Å, respectively (Wasastjerna *et al.*, 1923). Thus, 80CuNaY exhibits the highest response value toward the acetone vapor while 80FeNaY shows the lowest value. Moreover, another factor is the electron configuration of cation. Cu^{2+}, Ni^{2+}, and Fe^{2+} remain the unfilled electron state in the 3d orbital, only Cu^{2+} remains one unfilled electron state in 3d orbital as shown in Figure 5.2. Therefore Cu^{2+} is capable of rapidly accepting electrons which results in the increase in the proton mobility along the zeolite structure. Therefore, 80CuNaY exhibits the highest response to acetone vapor at the concentration of 30000 ppm relative to those of 80NiNaY and 80FeNaY, respectively. In the case of NaY, the electrical conductivity response and sensitivity of NaY are lower than those 80CuNaY and 80NiNaY due to the coordination number. Generally, the ion exchanged process between the monovalent and divalent electrons is that two units of monovalent cation are replaced with one unit of divalent cation. Hence, two units of Na^{+} are replaced with one unit of Cu^{2+} leading to the increase in the void size within 80CuNaY and the increase in the proton mobility (Yang *et al.*, 2007; Yimlamai *et al.*, 2011; Ji *et al.*, 2012; Kamonsawas *et al.*, 2012; Li *et al.*, 2012). In this work, 80CuNaY is used further to investigate the effects of dPPV and ketone vapor concentration and will be discussed next.

5.4.3.2 The Effect of Ketone Type

Figure 5.4 shows the plot between response and vapor concentration (ppm) of (5.4a) 80CuNaY, (5.4b) dPPV, and (5.4c) dPPV_[90]80CuNaY under acetone, MEK, and MIBK at 25 °C, 1 atm, and at vapor concentrations of 30000, 3000, 300, 30, and 10 ppm.

The electrical conductivity responses of 80CuNaY under acetone, MEK, and MIBK exposure at the vapor concentration of 30000 ppm are $6.74 \times 10^{-04} \pm 2.04 \times 10^{-05}$, $1.56 \times 10^{-04} \pm 1.88 \times 10^{-05}$, and $1.07 \times 10^{-04} \pm 2.75 \times 10^{-06}$, respectively. The electrical conductivity sensitivity of 80CuNaY in acetone, MEK and MIBK exposures at the vapor concentration of 30000 ppm are $5.00 \times 10^{-01} \pm 2.20 \times 10^{-02}$, $2.64 \times 10^{-01} \pm 5.25 \times 10^{-02}$, and $1.88 \times 10^{-01} \pm 5.95 \times 10^{-04}$, respectively as shown in Figure 5.4a and tabulated in Table 5.3. The electrical conductivity response and sensitivity of 80CuNaY depend on the solvent molecular size. For a large solvent molecular size, it is more difficult to penetrate into the zeolite framework. The size of acetone molecule is 0.524 nm which is smaller than the molecular sizes of MEK (0.667 nm) and MIBK (0.828 nm). Thus, the electrical conductivity response and sensitivity of 80CuNaY shows the highest values during the acetone exposure while during the MIBK exposure they show the lowest values (Yang *et al.*, 2007; Kamonsawas *et al.*, 2012). Figure 5.4b shows the plot of the dPPV vs. vapor concentration (ppm). The electrical conductivity response values of dPPV towards acetone, MEK, and MIBK vapors at the vapor concentration of 30000 ppm are $9.76 \times 10^{-02} \pm 2.05 \times 10^{-03}$, $3.17 \times 10^{-02} \pm 8.68 \times 10^{-03}$, and $1.66 \times 10^{-02} \pm 1.47 \times 10^{-04}$, respectively. The electrical conductivity sensitivity values of dPPV towards acetone, MEK, and MIBK vapors are $4.41 \pm 8.02 \times 10^{-01}$, $1.96 \pm 1.83 \times 10^{-01}$, and $1.00 \pm 9.95 \times 10^{-03}$, respectively as tabulated in Table 5.2. All of the electrical conductivity response and sensitivity values depend on the solvent molecular size, the same as 80CuNaY sample. When dPPV sample is exposed to acetone vapor, it shows high electrical conductivity response and sensitivity values when compared to those of MEK and MIBK vapors, respectively (Yang *et al.*, 2007; Kamonsawas *et al.*, 2012).

Figure 5.4c shows the plot of the electrical conductivity response of dPPV_[90]80CuNaY vs. vapor concentration (ppm). The electrical conductivity response of composite under acetone, MEK, and MIBK vapors at the

vapor concentration of 30000 ppm are 1.16 $x10^{-01}$ ± 4.74 $x10^{-03}$, 4.97 $x10^{-02}$ ± 5.30 $x10^{-03}$, and 2.41 $x10^{-02}$ ± 2.07 $x10^{-04}$, respectively. The electrical conductivity sensitivity values of the composite during acetone, MEK, and MIBK exposures at the vapor concentration of 30000 ppm are 4.98 ± 1.53 $x10^{-02}$, 2.51 = 5.72 $x10^{-02}$, and 1.70 ± 1.03 $x10^{-02}$, respectively. The electrical conductivity response and sensitivity also depend on the solvent molecular size, the same as the 80CuNaY and dPPV samples. The electrical conductivity response and sensitivity depend on the proton transfer along the zeolite framework: however dPPV has the conjugated double bond along the polymer chain leading to more electrons to transfer along the polymer chain, resulting in the higher values of the electrical conductivity response and sensitivity than that of the pristine 80CuNaY. Thus, after mixing dPPV into 80CuNaY matrix, the electrical conductivity response and sensitivity increase by an order magnitude as shown in Table 5.3 and Figure 5.4c (Li *et al.*, 2006; Wannatong *et al.*, 2008; Thongchai *et al.*, 2009; Arvand *et al.*, 2011 Chanthaanont *et al.*, 2012; Ji *et al.*, 2012; Kamonsawas *et al.*, 2012).

5.4.3.3 The Effect of Vapor Concentration

NaY, 80FeNaY, 80NiNaY, and 80CuNaY samples are investigated for the effect of vapor concentration. Figure 5.3 shows the plot between electrical conductivity responses vs. vapor concentration (ppm) of zeolite Y with four different transition cations in the zeolite framework. When the vapor concentration decreases, the electrical conductivity response and sensitivity of all samples also decrease. The minimum vapor concentration of 80CuNaY during acetone vapor exposure is 9 ppm. While 80NiNaY, NaY, and 80FeNaY can respond down to the minimum vapor concentrations of 12, 14, and 18 ppm, respectively as tabulated in Table 5.3. This is because both the cationic radii and the electron configuration combine to have an effect on the ability of the zeolite to respond to acetone vapor (Shannon *et al.*, 1976; Yang *et al.*, 2007; Li *et al.*, 2012).

Figure 5.4a is the plot between the response vs. vapor concentration of 80CuNaY and under the effect of ketone solvent type. The minimum vapor concentrations of acetone, MEK, and MIBK in which 80CuNaY are able to respond are 9, 18, and 20 ppm, respectively. This can be explained by the

solvent molecular size. Figure 5.4b shows the response of dPPV vs. vapor concentration. dPPV can respond the acetone, MEK, and MIBK minimum vapor concentrations of 5, 7, and 10 ppm, respectively. This is again attributed to the solvent molecular size effect, same as the 80CuNaY sample (Shannon *et al.*, 1976; Yang *et al.*, 2007; Soontornworajit *et al.*, 2007; Thongchai *et al.*, 2009; Ji *et al.*, 2012; Kamonsawas *et al.*, 2013).

DPPV is mixed into the 80CuNaY matrix at the ratio of 10% v/v of dPPV, dPPV has been shown to enhance the response of 80CuNaY. The minimum vapor concentrations in which composites can respond are further reduced to 5 ppm (acetone), 7 ppm (MEK), and 10 ppm (MIBK) as shown in Figure 5.4c and tabulated in Table 5.2 (Li *et al.*, 2006; Soontornworajit *et al.*, 2007; Thuwachaosoan *et al.*, 2007; Wannatong *et al.*, 2008; Thongchai *et al.*, 2009; Arvand *et al.*, 2011; Kamonsawas *et al.*, 2010; Chanthaanont *et al.*, 2012; Kamonsawas *et al.*, 2012; Kamonsawas *et al.*, 2013).

Comparing with other materials, NaY or zeolite Y (Na^+ and Si/Al=2.5) was exposed to DMMP vapor (Li *et al.*, 2010). The minimum vapor concentration was 20 ppm. For the process of ion-exchanged process in zeolite such as Cs-NaY and Cu-ZSM-5, they showed the lower minimum vapor concentration than NaY (Yang *et al.*, 2007; Urbiztondo *et al.*, 2009). Moreover, a conductive polymer such as polyaniline, as shown in Table 5.4, shows the high electrical conductivity response and a low vapor concentration towards methanol (Ayad *et al.*, 2009). It can be concluded that the ion exchanged process and the effect of conductive polymer can have dramatic effects on the response towards chemical vapors.

5.4.4 Investigations of the Adsorbed Acetone Vapor Interactions

5.4.4.1 Investigations the Interaction by FTIR

The interaction of zeolite Y and acetone vapor is investigated by the FTIR technique. The FTIR spectra of 80CuNaY (Figure 5.5) and dPPV_[90]80CuNaY (Figure 5.6) were taken in the 650-4000 cm^{-1} regions. The spectra were collected (a) before, (b) during exposure, and (c) after the acetone exposure.

Figure 5.5 shows the FTIR spectrum of 80CuNaY sample (5.5a) before, (5.5b) during, and (5.5c) after the acetone exposure. Before the acetone exposure, the adsorption peak of the Si-OH group (ν =3640 cm^{-1}) appears as one of the zeolite characteristics (Auerbach *et al.*, 2003; Yimlamai *et al.*, 2011; Kamonsawas *et al.*, 2012; Li *et al.*, 2012; Kamonsawas *et al.*, 2013). The characteristics of the tetrahedral unit are identified at 790, 1010, and 1150 cm^{-1} (Auerbach *et al.*, 2003; Kamonsawas *et al.*, 2012). The OH stretching which suggests the possibility of water in the zeolite structure is identified with the peak of 1600 cm^{-1} (Auerbach *et al.*, 2003; Yimlamai *et al.*, 2011; Kamonsawas *et al.*, 2012; Li *et al.*, 2012; Kamonsawas *et al.*, 2013). During the acetone exposure, the new peaks at 3449, 1734, and 1210 cm^{-1} can be assigned to the interaction between the carbonyl group of acetone molecule and the cation in the zeolite framework, as shown in Figure 5.7a (Biaglow *et al.*, 1993; Florian *et al.*, 1994; Fameth *et al.*, 1995; Hoost *et al.*, 1996; Panov *et al.*, 1998; Auerbach *et al.*, 2003; Martin *et al.*, 2008; Urbiztondo *et al.*, 2009; Yimlamai *et al.*, 2011; Boekfa *et al.*, 2012; Kamonsawas *et al.*, 2012; Li *et al.*, 2012; Kamonsawas *et al.*, 2013). After the acetone exposure, the IR spectrum peaks at 3449 and 1210 cm^{-1} evidently decrease; this confirms that the interaction between 80CuNaY and acetone vapor is not reversible.

Figure 5.6 shows the FTIR spectrum of dPPV_[90] 80CuNaY. Before the acetone exposure, the adsorption peak appears at 1150 cm^{-1} suggesting the quinoid structure, a characteristic of dPPV. The characteristics of the phenylene group appear as the peaks at 1514 and 3012 cm^{-1} (Ahlskog *et al.*, 1997; Kamonsawas *et al.*, 2010; Kamonsawas *et al.*, 2012; Kamonsawas *et al.*, 2013). The characteristic of the Si-OH group is at 3650 cm^{-1} (Auerbach *et al.*, 2003; Yimlamai *et al.*, 2011; Kamonsawas *et al.*, 2012; Li *et al.*, 2012; Kamonsawas *et al.*, 2013). During the acetone exposure, the new peaks at 3449 and 1210 cm^{-1} appear as the characteristic of H-O-C, suggesting an interaction between acetone and 80CuNaY (Biaglow *et al.*, 1993; Florian *et al.*, 1994; Fameth *et al.*, 1995; Hoost *et al.*, 1996; Panov *et al.*, 1998; Auerbach *et al.*, 2003; Martin *et al.*, 2008; Urbiztondo *et al.*, 2009; Yimlamai *et al.*, 2011; Boekfa *et al.*, 2012; Kamonsawas *et al.*, 2012; Li *et al.*, 2012; Kamonsawas *et al.*, 2013). The new peak at 1377 cm^{-1} indicates the characteristic of C-O; this also suggests an interaction between acetone and dPPV, as shown in Figure 5.7b. During

the acetone exposure, the intensity at 1150 cm^{-1} increases due to the increase in the number of the quinoid structures of dPPV (Ahlskog *et al.*, 1997; Kamonsawas *et al.*, 2010; Kamonsawas *et al.*, 2012; Kamonsawas *et al.*, 2013). After the acetone exposure, the intensities at 3012 and 1514 cm^{-1} decrease suggesting that the acetone molecule acts as a secondary dopant lead to increase the number of the quinoid structures in the dPPV chain (Ahlskog *et al.*, 1997; Kamonsawas *et al.*, 2010; Yimlamai *et al.*, 2011; Kamonsawas *et al.*, 2012; Kamonsawas *et al.*, 2013). The interaction is clearly irreversible.

The interaction of 80CuNaY with acetone vapor is shown in Figure 5.7a. The electron donating acetone molecule stabilizes the copper cation in the 80CuNaY. Thus, during the acetone exposure an electron on the acetone molecule can move along the 80CuNaY structure and increases the electrical conductivity (Auerbach *et al.*, 2003; Yimlamai *et al.*, 2011; Kamonsawas *et al.*, 2012; Li *et al.*, 2012; Kamonsawas *et al.*, 2013). When dPPV is mixed into the 80CuNaY matrix at the ratio of dPPV 10% v/v, acetone acts as an electron donating species for the 80CuNaY and dPPV structures during the acetone exposure as shown in Figure 5.7b. The lone pair electron of the carbonyl group of the acetone molecule stabilizes the cation along the dPPV structure resulting in greater negative charges corresponding to higher electrical conductivity when exposed to the acetone vapor (Ahlskog *et al.*, 1997; Kamonsawas *et al.*, 2010; Kamonsawas *et al.*, 2012; Kamonsawas *et al.*, 2013).

5.4.4.2 Investigations the Interaction by AFM

The interaction between dPPV[90]80CuNaY and acetone vapor is investigated by the phase changed by EFM mode under applied voltage at the tip of -8V. When applying a negative voltage at the tip, the material has a positive charge, and the bright area appears as shown because of the attractive force between the tip and the material. If the material has a negative charge, then it will show the dark area due to the repulsive force between the tip and the material. Before the acetone exposure, the phase image shows the bright area which suggests as the positive charge area as shown in Figure 5.8a. Figure 5.8c shows the plot between degree of charge generated vs. distance. The attractive force between the tip and the

dPPV_[90]80CuNaY sample before acetone exposure indicates that the sample have a lot of positive charges from the cation in zeolite frameworks.

After the acetone exposure. the phase image is changed to the dark area and the degree of charge generated decreases due to the repulsive force between dPPV_[90]80CuNaY and the tip because the active sites or positive charges react with the acetone vapor, as shown in Figures 5.8b and 5.8c. Before and after the acetone exposure, it is shown here that the phase image changes from bright area to dark area and the degree of charges generated changes by 20.7%.

5.5 Conclusions

The $CuCl_2$, $NiCl_2$, and $FeCl_2$ solutions were used for the ion exchanged NaY to prepare 80CuNaY, 80NiNaY, and 80FeNaY at 80% mole of cation. The highest electrical conductivity response and sensitivity when exposed to acetone vapor at vapor concentration of 30000 ppm belong to 80CuNaY in comparison to 80NiNaY, NaY, and 80FeNaY because of the proton mobility and electron configuration of cation in the zeolite structure. The large size of cation in the framework of zeolite led to a reduction in the electrostatic force between the framework and the cation, and the ease in which a proton can move. For the effect of vapor concentration, 80CuNaY could adsorb and respond to acetone vapor at the minimum vapor concentration of 9 ppm. When dPPV was mixed into the 80CuNaY matrix, the ability to adsorb and response decreased the minimum value to 5 ppm. For the effect of ketone vapor types, dPPV_[90]80CuNaY exposed to three different ketone vapors (acetone, MEK, and MIBK) at 3% v/v in N_2, the highest value of electrical conductivity response and sensitivity were obtained in the acetone exposure, whereas MIBK showed the lowest values due to the ability of the acetone molecule to penetrate into the zeolite framework. Thus, dPPV had been shown that it could enhance the electrical conductivity response and sensitivity of the 80CuNaY matrix. Moreover, under the acetone exposure the composite could respond to the acetone vapor at the lowest vapor concentration of 5 ppm whereas in the MIBK exposure the lowest vapor concentration is 10 ppm. The evidences of the irreversible interaction

between the active site and the acetone vapors were shown by the FTIR spectrum and AFM technique.

5.6 Acknowledgements

This work received financial support from The Conductive and Electroactive Polymers Research Unit of Chulalongkorn University; The Thailand Research Fund (TRF-RTA, TRF-RGJ PHD/0026/2553); and The Royal Thai Government Budget.

5.7 References

Ahlskog, M., Reghu, M., Noguchi, T., and Ohnishi, T. (1997) Doping and conductivity studies poly(p-phenylene vinylene). Synthetic Metals, 89, 11-15.

Arvand, M., Ansari, R., and Heydari, L. (2011) Development of a conductive composite based on polythiophene/Y-zeolite and its response towards sulfide ions. Materials Science and Engineering: C, 31, 1398-1404.

Ayad, M.M., Hefnawey, G.E., and Torad, N.L. (2009) A sensor of alcohol vapors based on thin polyaniline base film and quartz crystal microbalance. Journal of Hazardous Materials, 168, 85-88.

Auerbach, S.M., Carrado, K.A., and Dutta, P.K. (Eds.) (2003) Handbook of Zeolite Science and Technology. New York: Marcel Dekker.

Benvenho, A R.V., Li, R.W.C., and Gruber, J. (2009) Polymeric electronic gas sensor for determining alcohol content in automotive fuels. Sensors and Actuators B: Chemical, 136, 173-176.

Biaglow, A.I., Gorte, R.J., and David W. (1993) Molecular motions and 13C chemical shift anisotropy of acetone adsorbed in H-ZSM-5 zeolite. Journal of Physical Chemistry B, 97, 7135-713.

Boekfa, B., Pantu, P., Prosbt M., and Limtrakul, J. (2010) Adsorption and tautomerization reaction of acetone on acidic zeolites: the confinement

effect in different types of zeolites. Journal of Physical Chemistry C, 114, 15061-15067.

Chang, C.J., Lin, C.K., Chen, C.C., Chen, Y.C., and Kuo, E.H, (2011) Gas sensor with porous three dimensional framework using TiO_2/polymer double shell hollow microsphere. Thin Solid Films, 520, 1546-1553.

Chanthaanont, P. and Sirivat, A. (2012) Interaction of carbon monoxide with PEDOT-PSS/zeolite composite: effect of Si/Al ratio of ZSM-5 zeolite. e-Polymer, 12(1), 106-116.

Fameth, W.E., and Gorte, R.J. (1995) Methods for characterizing zeolite acidity. Chemical Reviews, 95, 615-635.

Florian, J., and Kubelkova, L. (1994) Proton transfer between H-Zeolite and adsorbed acetone or acetonitrile: quantum chemical and FTIR study. Journal of Physical Chemistry C, 98, 8734-8741.

Gao, J.F., Yan, D.X., Huang, H.D., Zeng, X.B., Zhang, W.Q., and Li, Z.M. (2011) Tunable positive liquid coefficient of an anisotropically conductive carbon nanotube-polymer composite. Journal of Polymer Research, 18, 2239-2243.

Heeger, A.J., and Diaz-Gracia, M.A. (1998) Semiconducting polymers as a material for photonic device. Current Opinion in Solid State Materials Science, 3, 16-22.

Hoost, T.E., Laframboise, K.A., and Otto, K. (1996) Infrared study of acetone and nitrogen oxides on Cu-ZSM-5. Catalysis Letters, 37, 153-156.

Hung, S.T., Chang, C.J., Hsu, C.H., Chu, B.H., Lo, C.F., Hsu, C.C., Pearton, S.J., and Holzworth, M.R., (2012) SnO_2 functionalized AlGaN/GaN high electron mobility transistor for hydrogen sensing application. International Journal of Hydrogen Energy, 37, 13783-13788.

Ji, X., Yao, W., Peng, J., Ren, N., Zhou, J., and Huang, Y. (2012) Evaluation of Cu-ZSM-5 zeolites as QCM sensor coatings for DMMP detection. Sensors and Actuators B: Chemical, 166-167, 50-55.

Jung, Y.S., Jung, W., Tuller, H.L., and Ross, C.A. (2008) Nanowire conductive polymer gas sensor patterned using self-assembled block copolymer lithography. Nano Letters, 8, 3776-3780.

Kamonsawas, J., Sirivat, A., Niamlang, S., Hormnirun, P., and Prissanaroon-Ouijai, W. (2010) Electrical conductivity response of poly(phenylene vinylene)/ zeolite composites exposed to ammonium nitrate. Sensors, 10, 5590-5603.

Kamonsawas, J., Sirivat, A., and Hormnirun, P. (2012) Poly(phenylene vinylene)/ zeolite Y composite as a ketone vapors sensor: effect of alkaline cations. Journal of Polymer Research, 19, 1-12.

Kamonsawas, J., Sirivat, A., and Hormnirun, P. (2013) Sensitive and selective responses of poly(phenylene vinylene)/zeolite Y-based sensors towards ketone vapors. International Journal of Polymeric Materials and Polymeric Biomaterials, 62:11, 583-589.

Li, X. and Dutta, P.K. (2010) Interaction of dimethylmethylphosphate with zeolite Y: impedance-based sensor for detecting nerve agent simulants. Journal of Physical Chemistry C, 114, 7986-7994.

Li, X. and Xue, D. (2006) Estimation of electronegativity values of elements in different valence states. Journal of Physical Chemistry A, 110, 11332-11337.

Martins, A.V.G., Berlier, G., Bisio, C., Coluccia, S., Pastore, H.O., and Marchese, L. (2008) Quantification of bronsed sites in microporous catalysts by a combined FTIR and NH_3-TPD study. Journal of Physical Chemistry C, 112, 7139-7120.

McKeen, J.C. and Davis, M.E. (2009) Conductivity of mono and divalent cation in the microporous zincosilicate VPI9. Journal of Physical Chemistry C, 113, 9870-9877.

Panov, A.G. and Fripiat, J.J. (1998) An infared study of acetone and mesityl oxide adsorption on acid catalyst. Langmuir, 14, 3788-3796.

Pirsa, S. and Alizadeh, N. (2012) A selective DMSO gas sensor based on nanostructured conducting polypyrrole doped with sulfonate anion. Sensors and Actuators B: Chemical, 168, 303-309.

Ruangchuay, L., Sirivat, A., and Schwank, J. (2004) Selective conductivity response of polypyrrole-based sensor on flammable chemicals. Reactive and Functional Polymers, 61, 11-22.

Satsuma, A., Yang, D., and Shimizu, K.I. (2011) Effect of pore diameter of zeolites on detection of base molecules by zeolite thick film sensor. Microporous and Mesoporous Materials, 141, 20-25.

Shannon. R.D. (1976) Revised effective ionic radii and systematic studies of interatomic distances in halides and chalcogenides. Acta Crystallographica Section A, 32, 751-767.

Soontornworajit, B., Wannatong, L., Hiamtup, P., Niamlang, S., Chotpattananont, D., Sirivat, A., and Schwank, J. (2007) Induced interaction between polypyrrole and SO_2 via molecular sieve 13X. Materials Science and Engineering: B, 15, 78-86.

Tang, Li., Li, Y., Xu, K., Hou, X., and Lv, Y. (2008) Sensitive and selective acetone sensor based on its cataluminescence from Nano-La_2O_3 surface. Sensors and Actuators B: Chemical, 132, 243-249.

Thongchai, N., Kunanuruksapong, R., Niamlang, S., Wannatong, L., Sirivat, A., and Wongkasemjit, S. (2009) Interactions between CO and poly(p-phenylene vinylene) as induced by ion-exchanged zeolites. Materials, 2, 2259-2275.

Thuwachaosoan, K., Chottananont, D., Sirivat, A., Rujiravanit, R., and Schwank, J. (2007) Electrical conductivity responses and interactions of poly(3-thiopheneacetic acid)/zeolites L, mordenite, beta, and H_2. Materials Science and Engineering: B, 140, 23-30.

Urbiztondo, M.A., Pellejero, I., Villarroya, M., Sese, J., Pina, M.P., Dufour, I., and Santamaría, J. (2009) Zeolite-modified cantilevers for the sensing of nitrotoluene vapors. Sensors and Actuators B: Chemical, 137, 608-616.

Urbiztondo, M.A., Peralta, A., Pellejero, I., Sese, J., Pina M.P., Dufour, I., and Santamaria, J. (2012) Detection of organic vapors with Si cantilevers coated with inorganic (zeolite) or organic (polymer) layers. Sensors and Actuators B: Chemical, 171-172, 822-831.

Varsani, P., Afonja, A., Williams, D.E., Parkin, I.P., and Binions, R. (2011) Zeolite-modified WO3 gas sensors-enhanced detection of NO_2. Sensors and Actuators B: Chemical, 160, 475-482.

Vijaya, J.J., Kenedy, L.J., Sekaran, G., Bayhan, M., and William, M. (2008) Preparation and VOC gas sensing properties of Sr(II)-added copper aluminate spinel composites. Sensors and Actuators B: Chemical, 134, 604-612.

Wannatong, L., Sirivat, A., and Schwank, J. (2008) Polypyrrole and its composites with 3A zeolite and polyamide 6 as sensors for four chemicals in lacquer thinner. Reactive and Functional Polymers, 68, 1646-1651.

Wasastjerna, J. (1923) On the radii of ions. Societas Scientiarum Fennica, 1(38), 1-25.

Wessling, R.A. and Zimmerman, R.G. (1968) Polyelectrolytes from bis-sulfonium salts. U.S.Patent, 3, 401.

Yang, P., Ye, X., Lau, C., Li, Z., Liu, X., and Lu, J. (2007) Design of efficient zeolite sensor materials for n-hexane. Analytical Chemistry, 79, 1425-1432.

Yimlamai, I., Niamlang, S., Chanthaanont, P., Kunanuruksapong, R., Changkhamchom, S., and Sirivat, A. (2011) Electrical conductivity response and sensitivity of ZSM-5, Y and mordenite zeolite towards ethanol vapor. Ionics, 17, 607-615.

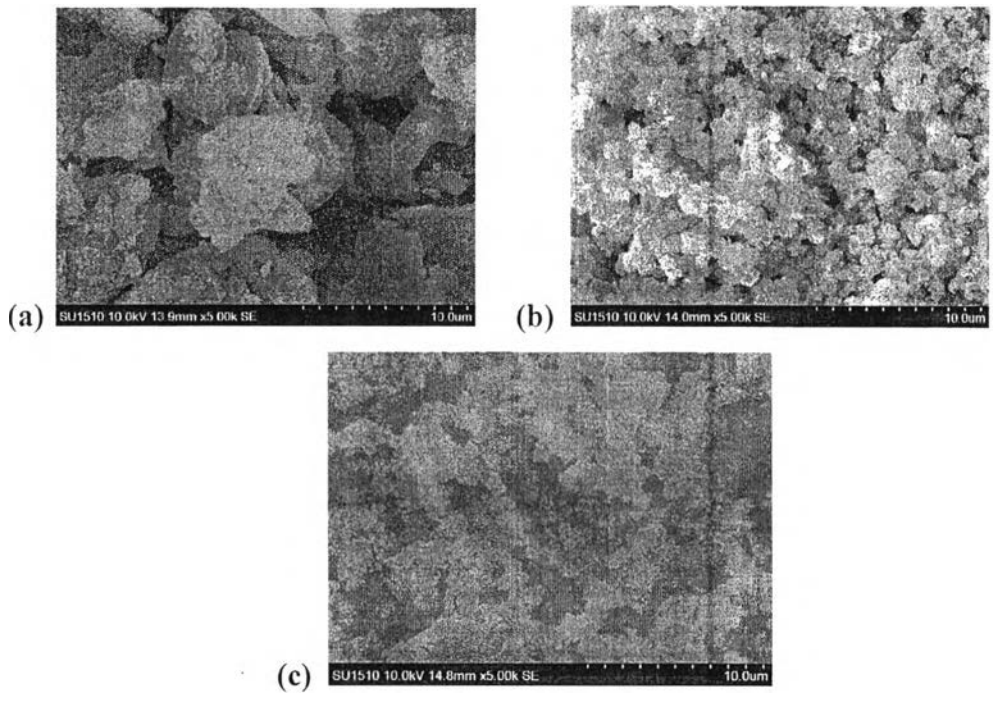

Figure 5.1 The morphology of dPPV, 80CuNaY powders and dPPV_[90]80CuNaY composites with 10% v/v of dPPV: (a) dPPV at magnification of 5000; (b) 80CuNaY at magnification 5000; and (c) dPPV_[90]80CuNaY at magnification of 5000.

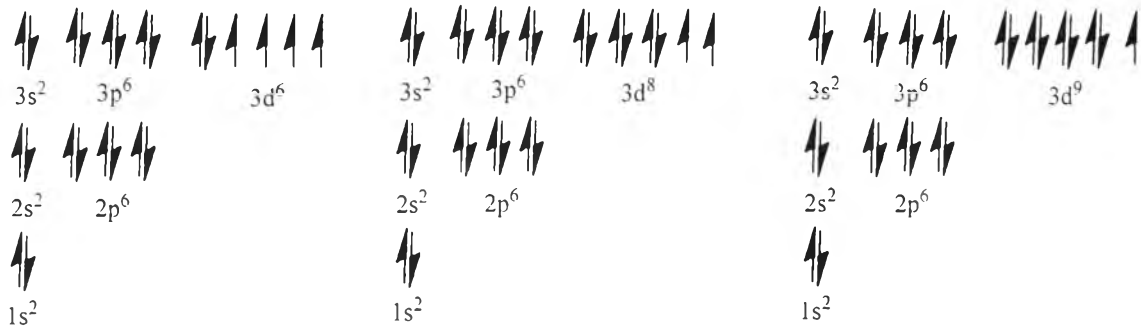

Cation	Fe^{2+}	Ni^{2+}	Cu^{2+}
EN	1.292	1.367	1.372
Cationic radii (Å)	0.75	0.83	0.87

Figure 5.2 The electron orbitals of Fe^{2+}, Ni^{2+}, and Cu^{2+}.

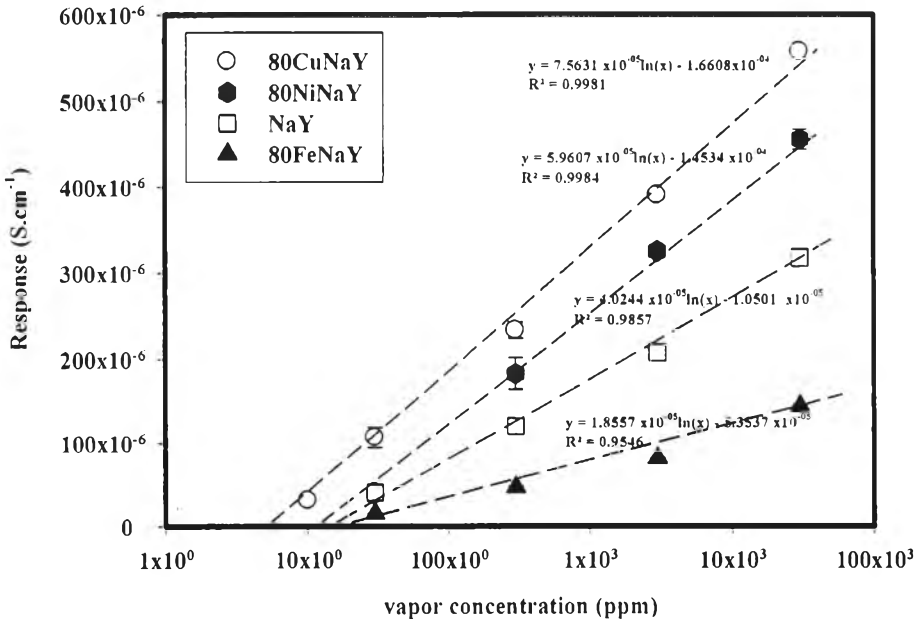

Figure 5.3 Electrical conductivity response of the NaY, 80CuNaY, 80NiNaY, and 80FeNaY under acetone exposure at 25 °C, 1 atm, at vapor concentrations of 30000, 3000, 300, 30, and 10 ppm.

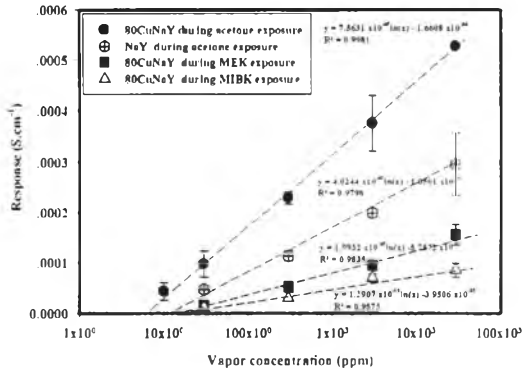

(a) 80CuNaY

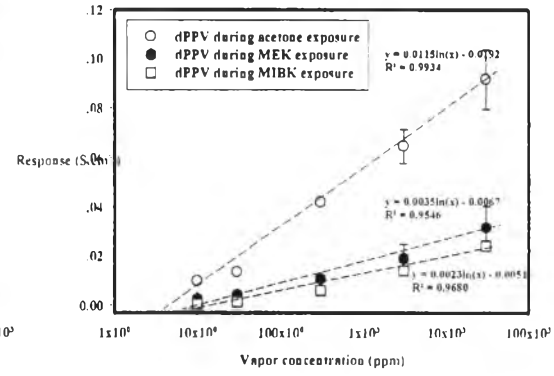

(b) dPPV

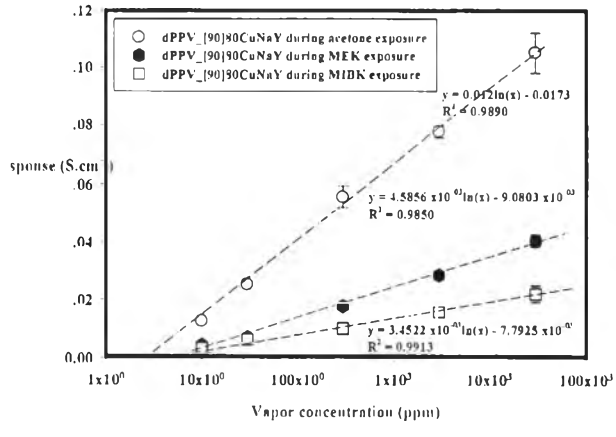

(c) dPPV_[90]80CuNaY

Figure 5.4 Electrical conductivity response of: (a) 80CuNaY; (b) dPPV; and (c) dPPV_[90] 80CuNaY under acetone, MEK, and MIBK exposures at 25 °C, 1 atm, at vapor concentrations of 30000, 3000, 300, 30, and 10 ppm.

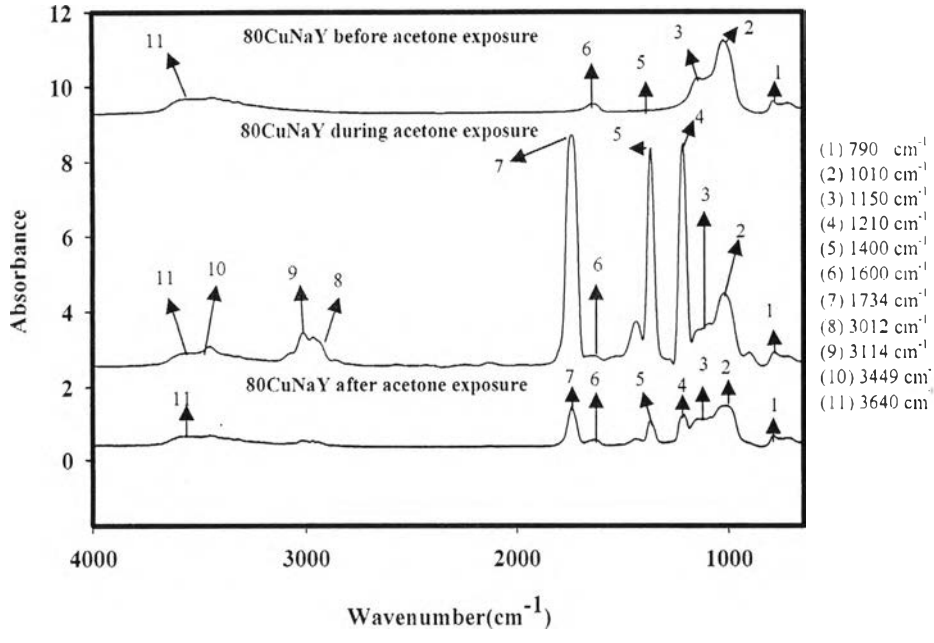

Figure 5.5 FTIR spectra of 80CuNaY exposed to acetone at vapor concentration of 30000 ppm (at pressure of 1 atm and at T=25°C).

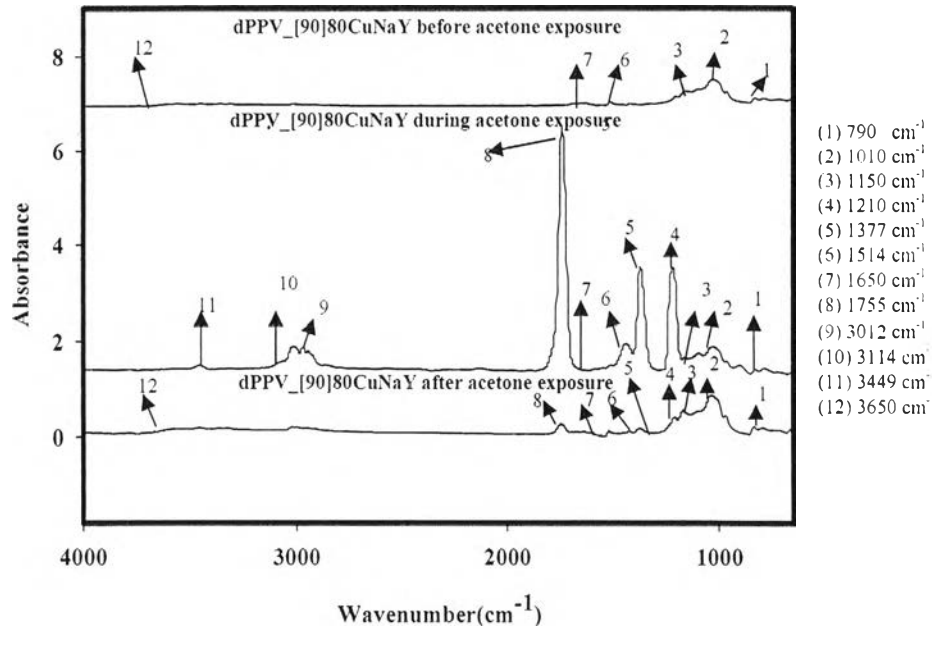

Figure 5.6 FTIR spectra of dPPV_[90]80CuNaY exposed to acetone at vapor concentration of 30000 ppm (at pressure of 1 atm and T=25 °C).

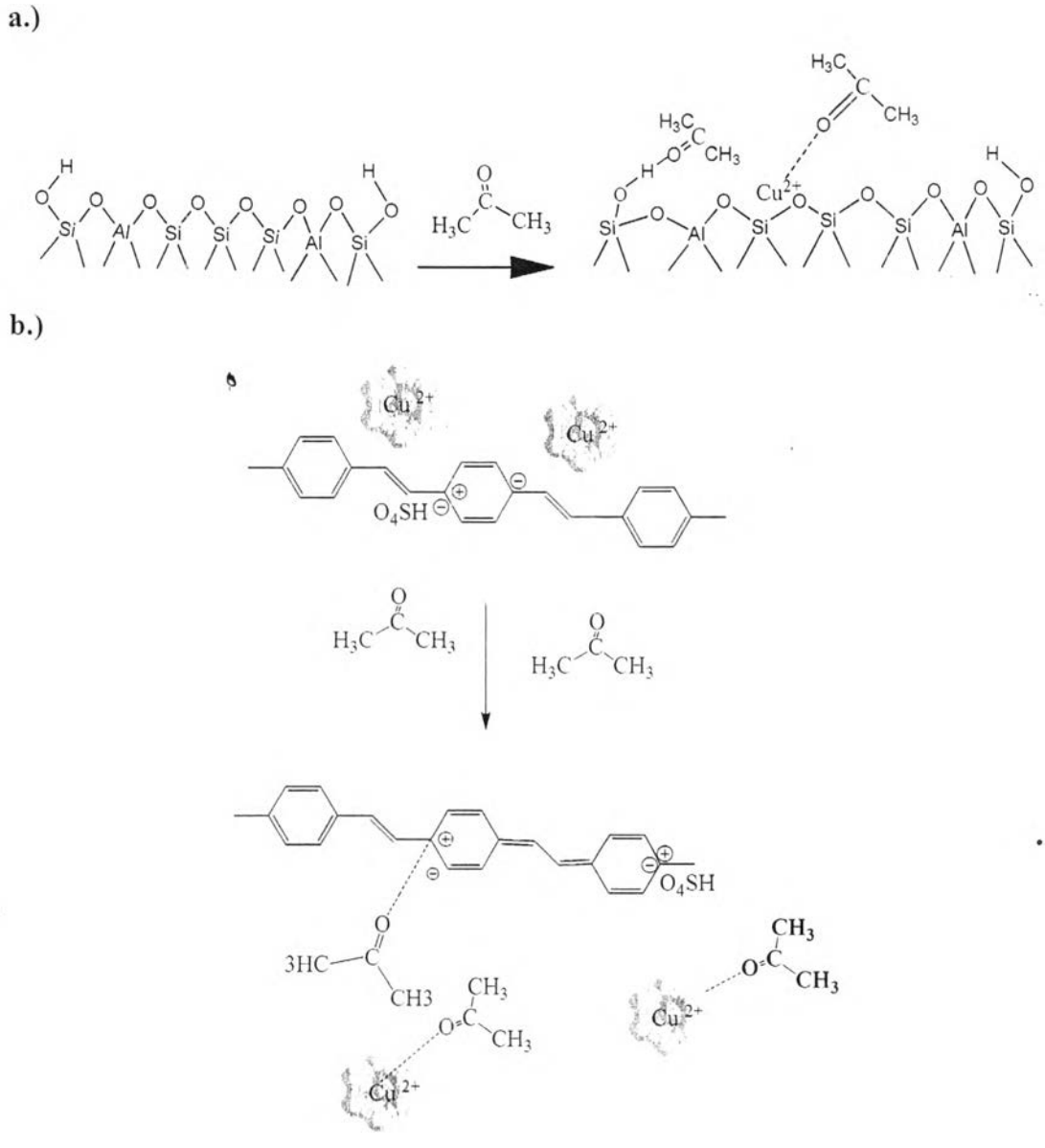

Figure 5.7 Interactions between acetone vapor and: (a) 80CuNaY; and (b) dPPV_[90]80CuNaY.

Before Acetone Exposure **After Acetone Exposure**

Phase Image

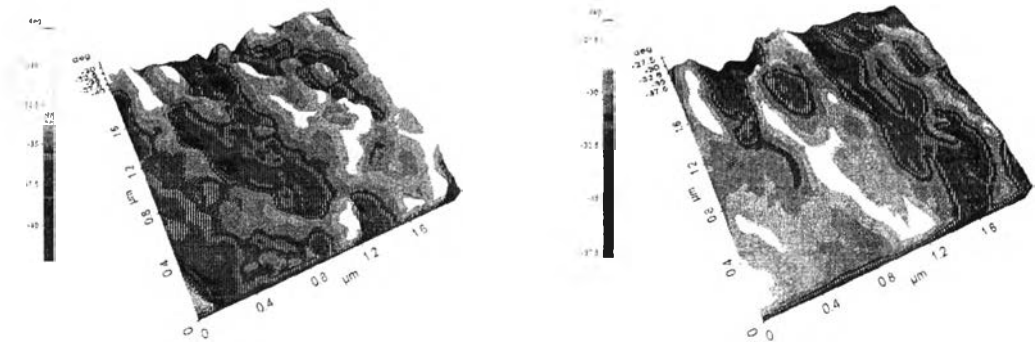

(8a) At 25 °C, Sample bias -8V (8b) At 25 °C, Sample bias -8V

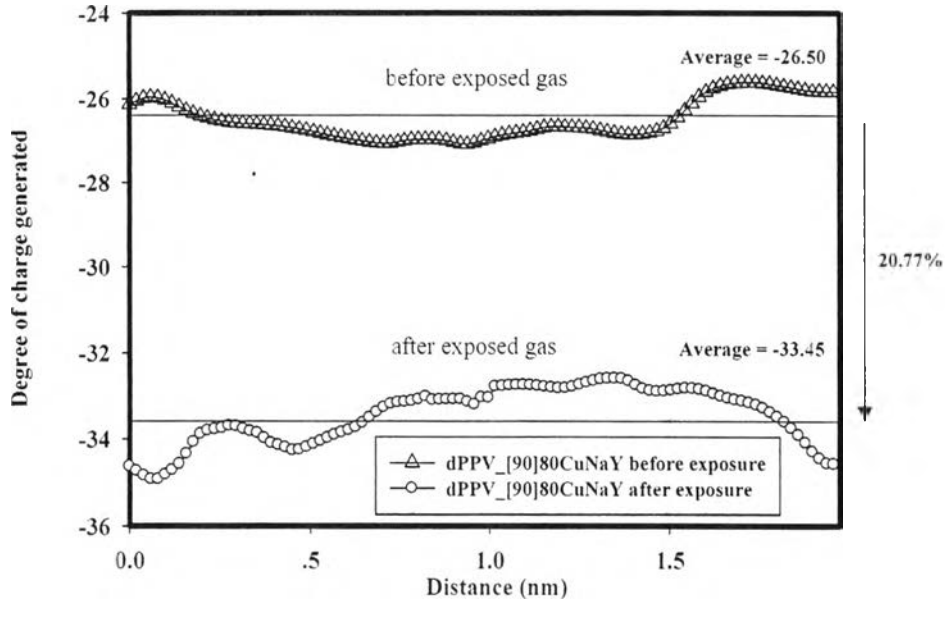

(8c)

Figure 5.8 EFM-Phase images of: (a) dPPV_[90]80CuNaY before exposure; (b) during acetone exposure; and (c) degree of charges generated on dPPV_[90] 80CuNaY under -8 V of tip bias across the whole region.

Table 5.1 Analytical data and electrical conductivity of modified zeolite Y

Sample	Sample Code	% Mole of Cation	EN	Cationic Radii (Å)	Median Pore Width (Å)	Surface Area (m^2/g)	σ_{air} (S/cm)
Zeolite Y (Si/Al =5.1 and Na^+)	NaY	100% Na^+	0.93 (Na^+)	1.16 (Na^+)	7.4875 ± 0.34	617.0 ± 7.0	$2.50 \times 10^{-3} \pm 2.51 \times 10^{-5}$
Zeolite Y (Si/Al =5.1, Na^+, and Cu^{2+})	80CuNaY	79% Cu^{2+} and 21% Na^+	0.93 (Na^+) and 1.372 (Cu^{2+})	1.16 (Na^+) and 0.87 (Cu^{2+})	7.092 ± 0.04	526.0 ± 2.0	$5.67 \times 10^{-3} \pm 7.08 \times 10^{-5}$
Zeolite Y (Si/Al =5.1, Na^+, and Ni^{2+})	80NiNaY	84% Ni^{2+} and 16% Na^+	0.93 (Na^+) and 1.367 (Ni^{2+})	1.16 (Na^+) and 0.83 (Ni^{2+})	7.656 ± 0.03	506.0 ± 6.0	$3.51 \times 10^{-3} \pm 1.15 \times 10^{-6}$
Zeolite Y (Si/Al =5.1, Na^+, and Fe^{2+})	80FeNaY	90% Fe^{2+} and 10% Na^+	0.93 (Na^+) and 1.292 (Fe^{2+})	1.16 (Na^+) and 0.75 (Fe^{2+})	7.326 ± 0.39	535.0 ± 4.0	$2.44 \times 10^{-3} \pm 1.66 \times 10^{-5}$

Table 5.2 The induction and recovery times of modified zeolite Y, dPPV, and composites

Sample	Sample Code	Ketone Type	Induction Time, Ti (min) at Vapor Concentration of					Recovery Time, Tr (min) at Vapor Concentration of				
			10 ppm	30 ppm	300 ppm	3000 ppm	30000 ppm	10 ppm	30 ppm	300 ppm	3000 ppm	30000 ppm
Doped PPV	dPPV	acetone	15 ± 0.3	15 ± 0.6	18 ± 0.8	20 ± 0.5	35 ± 0.2	11 ± 0.1	11 ± 0.2	13 ± 0.5	13 ± 0.2	20 ± 1.0
Zeolite Y (Si/Al = 5.1 and Na^+)	NaY		-	22 ± 0.5	27 ± 1.0	34 ± 0.8	42 ± 2.0	-	10 ± 3.0	12 ± 2.0	20 ± 0.3	27 ± 2.0
Zeolite Y (Si/Al = 5.1, Na^+, and Cu^{2+})	80CuNaY		19 ± 1.0	20 ± 1.0	21 ± 3.0	23 ± 2.0	38 ± 1.0	10 ± 4.0	15 ± 1.0	18 ± 2.0	23 ± 4.0	31 ± 2.0
Zeolite Y (Si/Al = 5.1, Na^+, and Ni^{2+})	80NiNaY		-	21 ± 1.0	23 ± 1.0	29 ± 2.0	40 ± 1.0	-	16 ± 1.0	16 ± 2.0	23 ± 1.0	32 ± 1.0
Zeolite Y (Si/Al = 5.1, Na^+, and Fe^{2+})	80FeNaY		-	24 ± 2.0	29 ± 2.0	36 ± 2.0	45 ± 1.0	-	19 ± 2.0	21 ± 1.0	25 ± 2.0	38 ± 1.0
10%v/v of dPPV_ zeolite Y (Si/Al = 5.1, Na^+, and Cu^{2+})	dPPV_[90] 80CuNaY		15 ± 2.0	16 ± 1.0	18 ± 0.8	18 ± 2.0	36 ± 1.0	10 ± 0.5	12 ± 1.0	12 ± 2.0	25 ± 1.0	26 ± 2.0

Table 5.2 The induction and recovery times of modified zeolite Y, dPPV, and composites (continue)

Sample	Sample Code	Ketone Type	Induction Time, Ti (min) at Vapor Concentration of					Recovery Time, Tr (min) at Vapor Concentration of				
			10 ppm	30 ppm	300 ppm	3000 ppm	30000 ppm	10 ppm	30 ppm	300 ppm	3000 ppm	30000 ppm
Doped PPV	dPPV	MEK	-	12 ± 1.0	13 ± 2.0	18 ± 1.0	32 ± 2.0	-	9 ± 1.0	9 ± 2.0	10 ± 1.0	11 ± 2.0
Zeolite Y ($Si/Al = 5.1$, Na^{+}, and Cu^{2+})	80CuNaY		-	16 ± 1.0	17 ± 2.0	20 ± 1.0	35 ± 2.0	-	11 ± 1.0	11 ± 3.0	11 ± 1.0	13 ± 1.0
10%v/v of dPPV_zeolite Y ($Si/Al = 5.1$, Na^{+}, and Cu^{2+})	dPPV_[90] 80CuNaY		-	13 ± 1.0	15 ± 2.0	18 ± 1.0	31 ± 1.0	-	9 ± 1.0	10 ± 0.5	10 ± 1.0	12 ± 2.0
Doped PPV	dPPV	MIBK	-	9 ± 1.0	10 ± 1.0	10 ± 2.0	12 ± 0.5	-	6 ± 2.0	6 ± 1.0	9 ± 1.0	10 ± 1.0
Zeolite Y ($Si/Al = 5.1$, Na^{+}, and Cu^{2+})	80CuNaY		-	16 ± 1.0	16 ± 2.0	17 ± 1.0	18 ± 2.0	-	9 ± 2.0	10 ± 1.0	12 ± 1.0	12 ± 1.0
10%v/v of dPPV_zeolite Y ($Si/Al = 5.1$, Na^{+}, and Cu^{2+})	dPPV_[90] 80CuNaY		-	15 ± 0.5	15 ± 2.0	16 ± 2.0	17 ± 2.0	-	6 ± 0.7	9 ± 2.0	11 ± 1.0	11 ± 2.0

Table 5.3 The response and sensitivity of modified zeolite Y, dPPV, and composites

Sample	Chemical Vapor	Response (S/cm)*	Sensitivity*	Minimum Vapor Concentration (ppm)
80FeNaY	acetone	$1.49 \times 10^{-04} \pm 2.16 \times 10^{-06}$	$2.38 \times 10^{-01} \pm 1.66 \times 10^{-02}$	18
NaY	acetone	$3.23 \times 10^{-04} \pm 9.95 \times 10^{-05}$	$2.64 \times 10^{-01} \pm 2.05 \times 10^{-02}$	14
80NiNaY	acetone	$4.62 \times 10^{-04} \pm 8.06 \times 10^{-06}$	$3.53 \times 10^{-01} \pm 1.93 \times 10^{-02}$	12
80CuNaY	acetone	$6.74 \times 10^{-04} \pm 2.04 \times 10^{-05}$	$5.00 \times 10^{-01} \pm 2.20 \times 10^{-02}$	9
80CuNaY	MEK	$1.56 \times 10^{-04} \pm 1.88 \times 10^{-03}$	$2.64 \times 10^{-01} \pm 5.25 \times 10^{-02}$	18
80CuNaY	MIBK	$1.07 \times 10^{-04} \pm 2.75 \times 10^{-06}$	$1.88 \times 10^{-01} \pm 5.59 \times 10^{-04}$	20
dPPV	acetone	$9.76 \times 10^{-02} \pm 2.05 \times 10^{-03}$	$4.41 \pm 8.02 \times 10^{-01}$	5
dPPV	MEK	$3.17 \times 10^{-02} \pm 8.68 \times 10^{-03}$	$1.96 \pm 1.83 \times 10^{-01}$	7
dPPV	MIBK	$1.66 \times 10^{-02} \pm 1.47 \times 10^{-04}$	$1.00 \pm 9.95 \times 10^{-03}$	9
dPPV_[90]80CuNaY	acetone	$1.16 \times 10^{-01} \pm 4.74 \times 10^{-03}$	$4.98 \pm 1.53 \times 10^{-02}$	5
dPPV_[90]80CuNaY	MEK	$4.97 \times 10^{-02} \pm 5.30 \times 10^{-03}$	$2.51 \pm 5.72 \times 10^{-02}$	7
dPPV_[90]80CuNaY	MIBK	$2.41 \times 10^{-02} \pm 2.07 \times 10^{-04}$	$1.70 \pm 1.03 \times 10^{-02}$	10

* The response and sensitivity of gas sensing materials at vapor concentration of 30000 ppm

Table 5.4 Comparison with other materials

Materials	Method	Vapor Type	Minimum Vapor Concentration (ppm)	References
NaY	LCR meter	DMMP	20	Li *et al.*, (2010)
CsNaY	TCL	n-hexane	0.43	Yang *et al.*, (2007)
Cu-ZSM-5	QCM	DMMP	0.1	Li *et al.*, (2012)
Co-BEA	LCR meter	ethanol	66	Urbiztondo *et al.*, (2009)
Polyaniline	QCM	methanol	9	Ayad *et al.*, (2009)
dPPV_[90]80CuNaY	Conventional 2-point probe	acetone	5	This recent work